Supplementary Information for:

Mechanisms for maintaining cell shape in rod-shaped Gram-negative bacteria

### Leon Furchtgott[1,†], Ned S. Wingreen[2], Kerwyn Casey Huang[1,*]

[1]Department of Bioengineering, 318 Campus Drive West, Stanford University, Stanford, CA 94305.

[2]Department of Molecular Biology, Washington Road, Princeton University, Princeton, NJ 08544.

[†]Current address: Biophysics Program, Harvard University, Cambridge, MA 02138.

[*]: To whom correspondence should be addressed.

Address: Department of Bioengineering
318 Campus Drive West, Stanford University
Stanford, CA 94305 USA
E-mail: kchuang@stanford.edu
Phone: (650) 721-2483; Fax: (650) 724-1922.
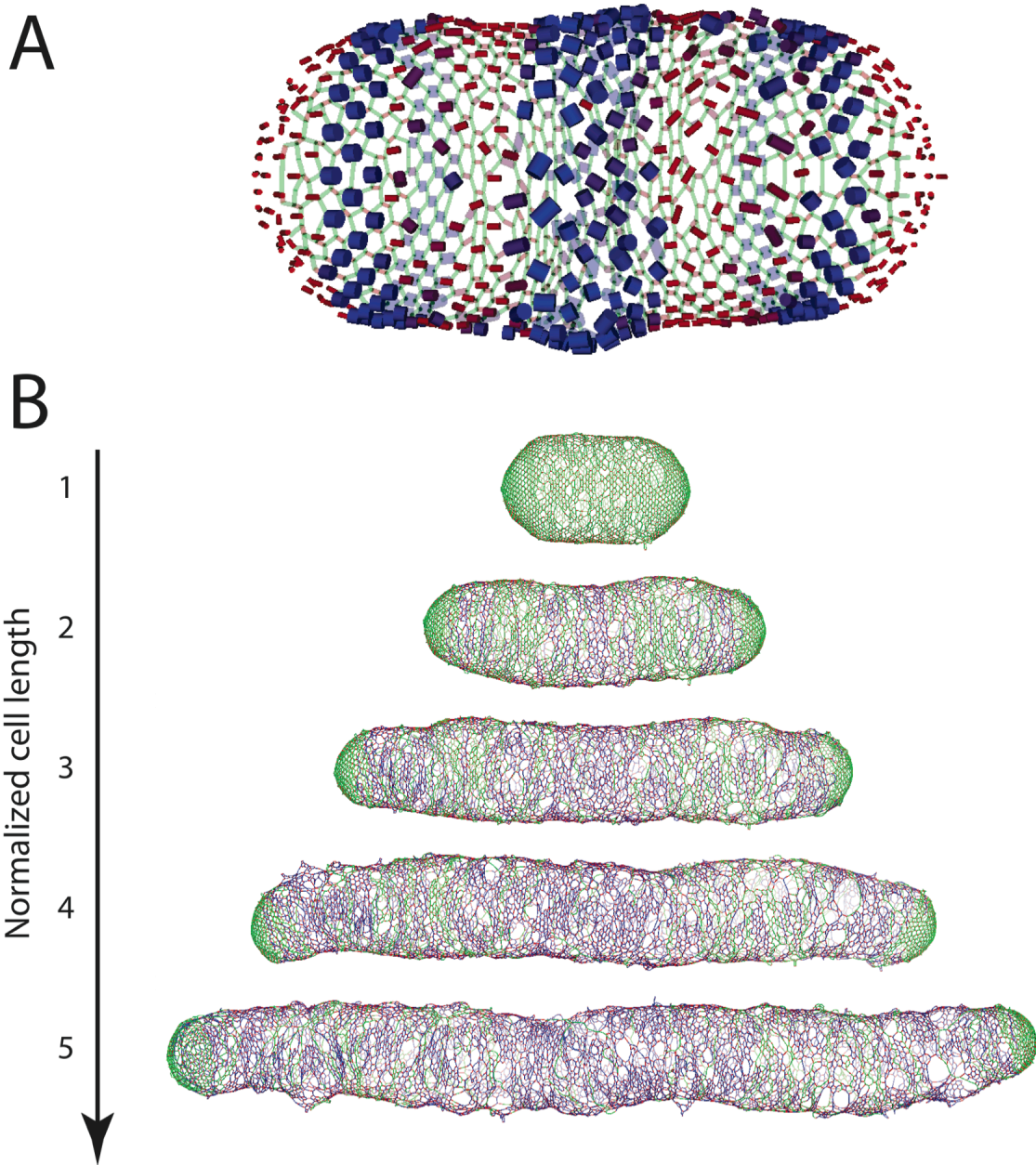
Supplemental Figure 1: Rod shape is maintained with a pattern of insertion mimicking FtsZ-mediated elongation. (A) Schematic of insertion pattern with increased probability of insertion near the poles and near midcell. The probability of insertion in the cylindrical regions within $L/8$ of the poles or midcell is doubled relative to the uniform insertion model in Fig. 2F. (B) Cell wall grown to five times its original length.
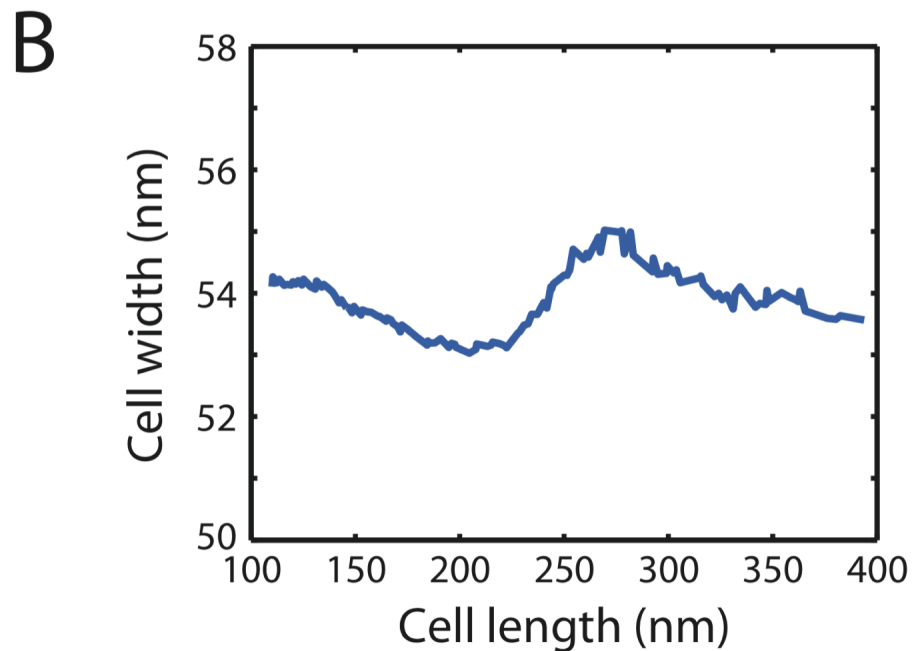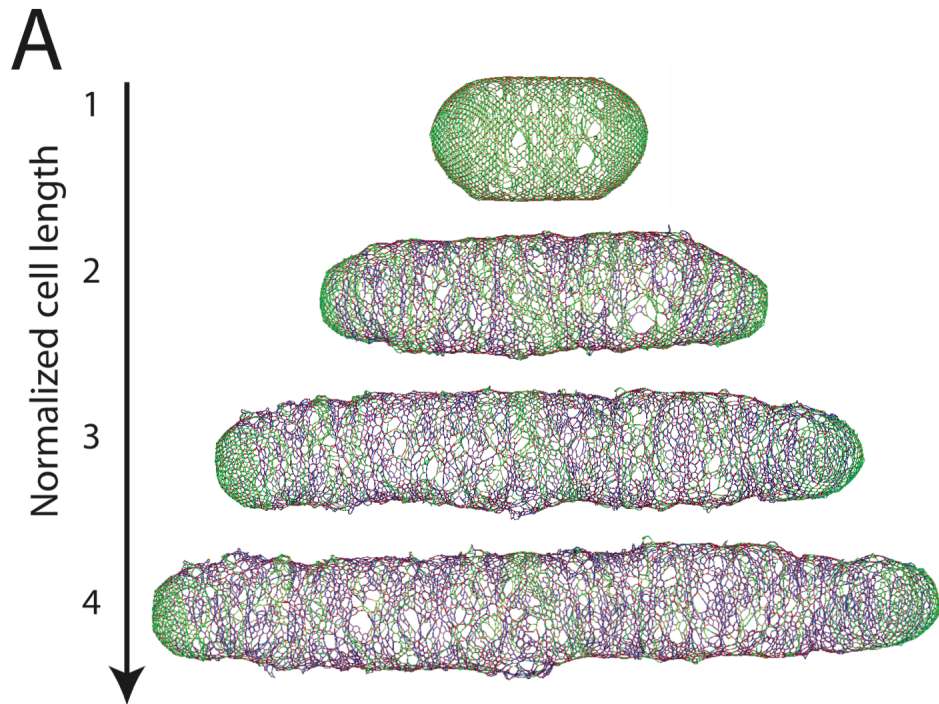
Supplemental Figure 2: Cell width is preserved with insertional stretching and a Gaussian distribution of inserted strand lengths. (A) Cell walls grown with uniform insertion to four times their original length, with 10% insertional stretching and inserted strands with a Gaussian distribution of lengths with mean 20 and standard deviation 5. (B) Average local width as a function of length for the last cell in A.
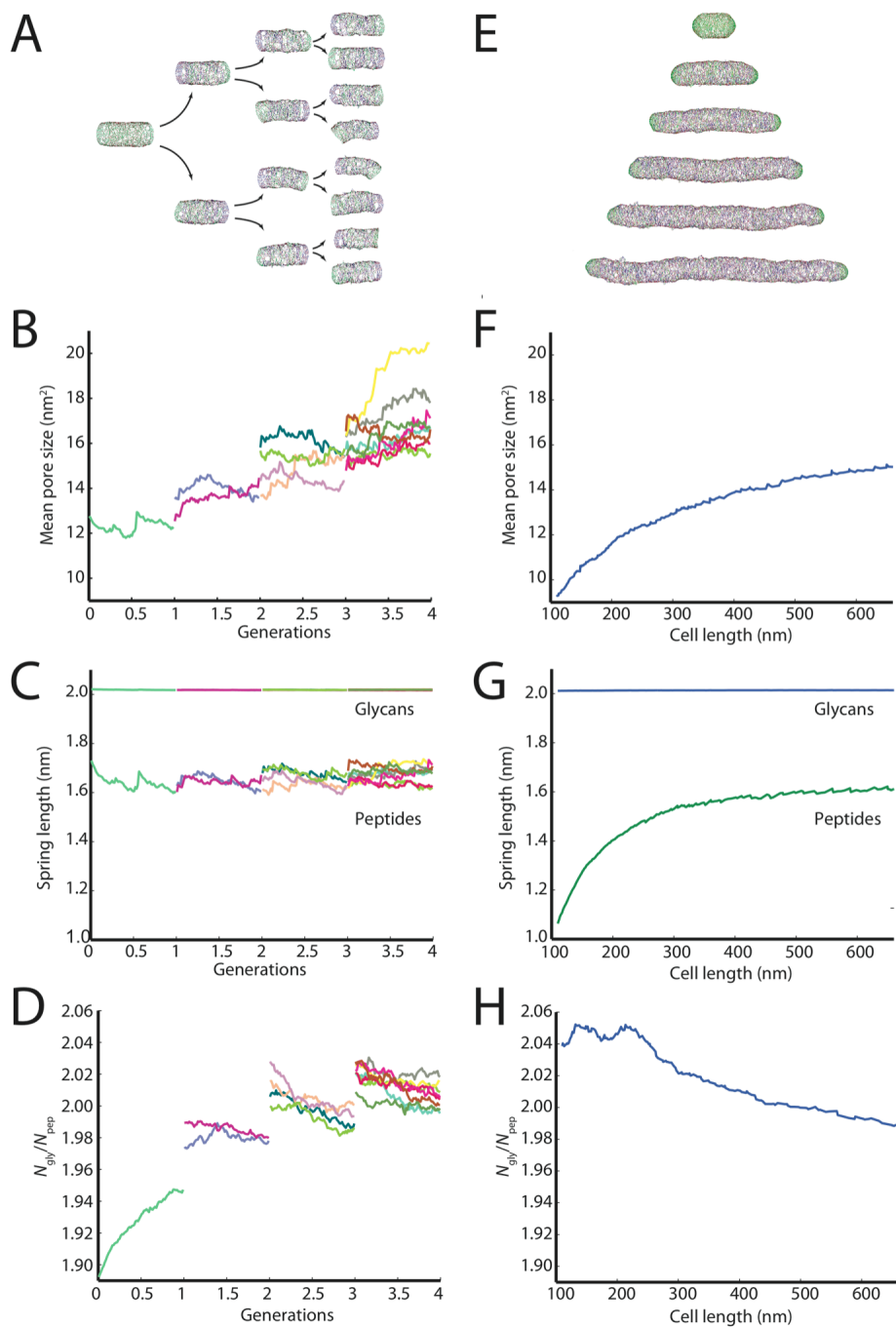
Supplemental Figure 3: Metrics of cell-wall network organization converge to steady-state values. (A,E) Simulations of 3 cycles of growth and division from Fig. 4A (A) and of a cell wall grown to six times its original length (E). Both sets of simulations use the uniform-insertion model with $L = 20$ and 10% stretching. In both cases, key metrics of average cell-wall organization converge to common steady-state values: (B,F) Average pore size. (C,G) Average peptide and glycan length. (D,H) Ratio of the number of glycans to the number of peptides (a fully crosslinked, single-layer cell wall without defects has a ratio of 2).
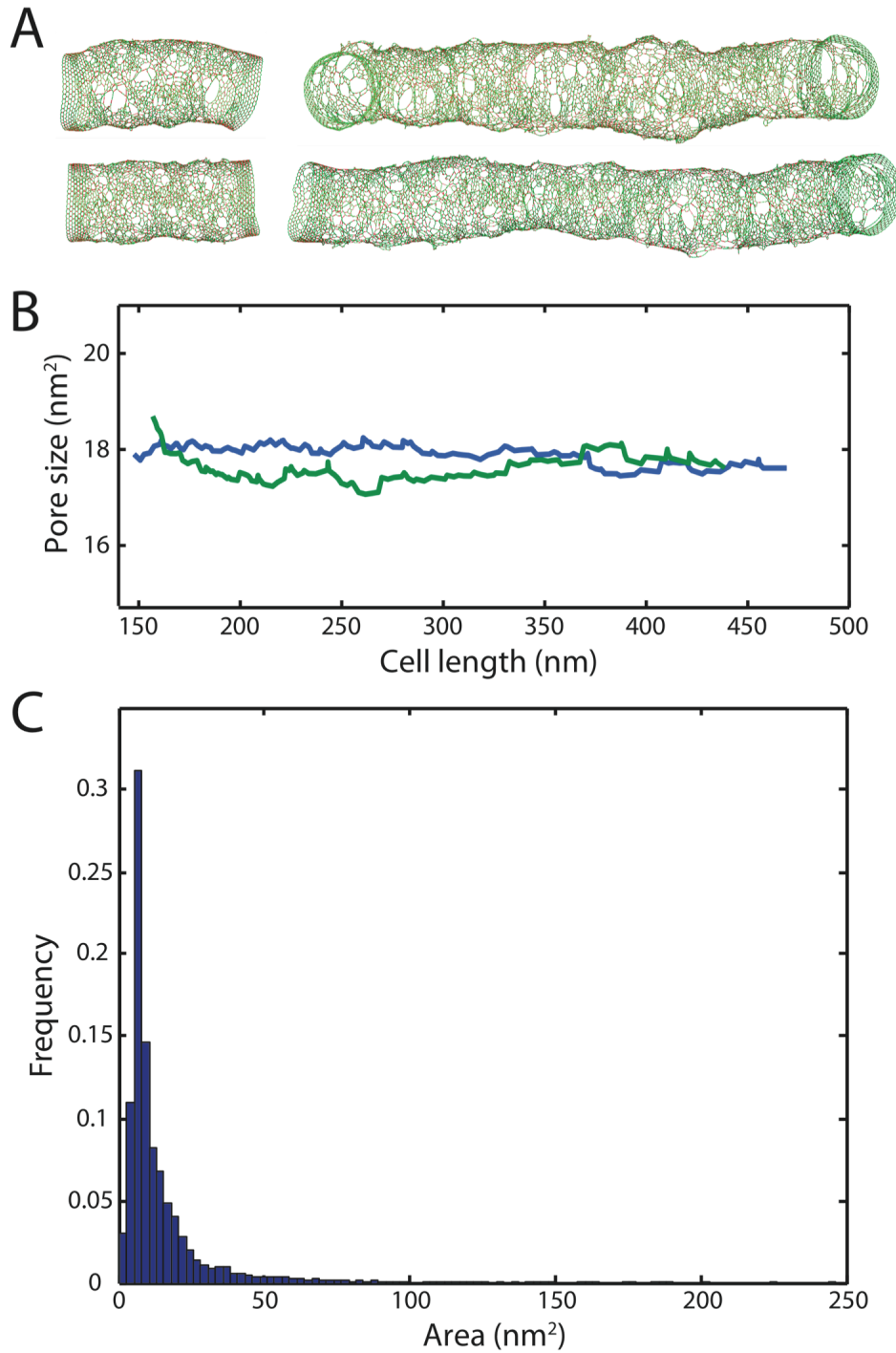
Supplemental Figure 4: Average cell-wall pore size converges to a steady-state value. (A) Two cells selected from the fourth generation in Fig.~4 grown to three times their original length using the uniform insertion model. (B) Average pore size as a function of length for the cells in A. (C) Steady-state distribution of pore sizes.
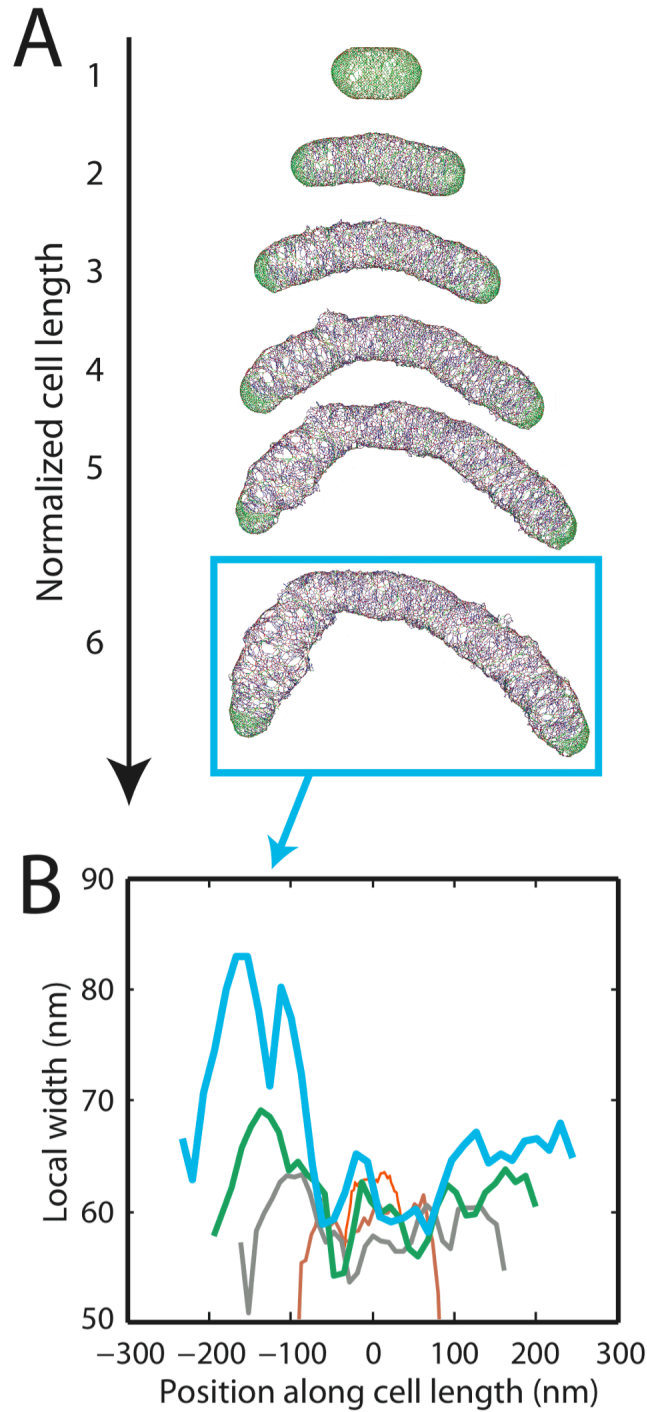
Supplemental Figure 5: Insertional stretching does not prevent loss of cell shape during growth with the random-insertion model. (A) Cell wall grown to six times its original length using the random-insertion model (similar to Fig. 2B) with L = 20 and 10% stretching. Cells still undergo severe bending and bulging. (B) Local width of cell walls in A.
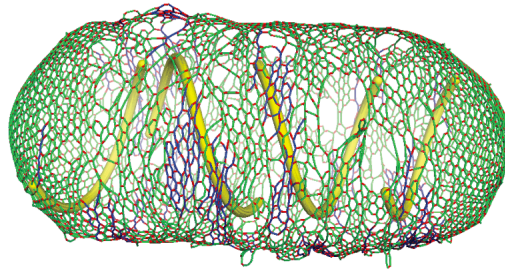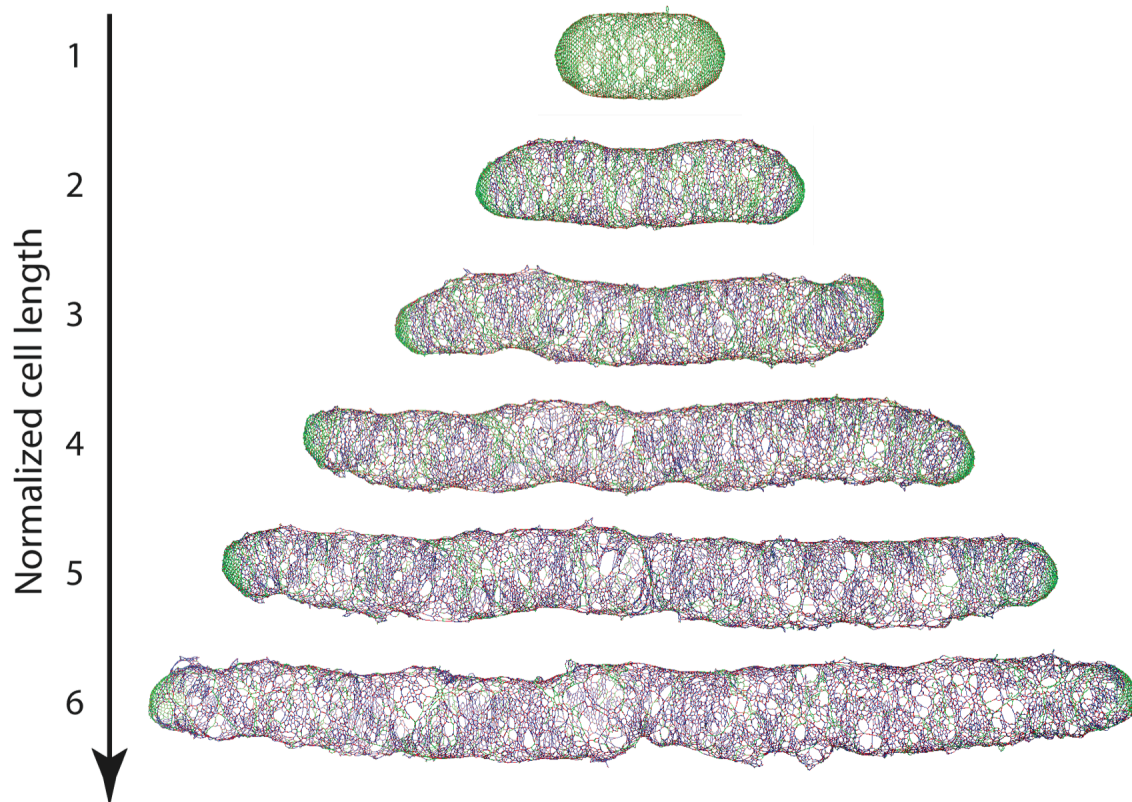
Supplemental Figure 6: Rod shape is maintained with a pattern of insertion mimicking short, treadmilling filaments. (A) Schematic of insertion pattern during one stage of growth. Helical filaments (yellow) determine the allowed sites of insertion. Filaments elongate independently as the cell wall grows, and randomly orient relative to the cell-wall network every time the length increases by 33%. (B) Cell wall grown to six times its original length.

A helical angle = 30 degrees

B

Normalized cell length

1.0

1.5

2.0

2.5

3.0
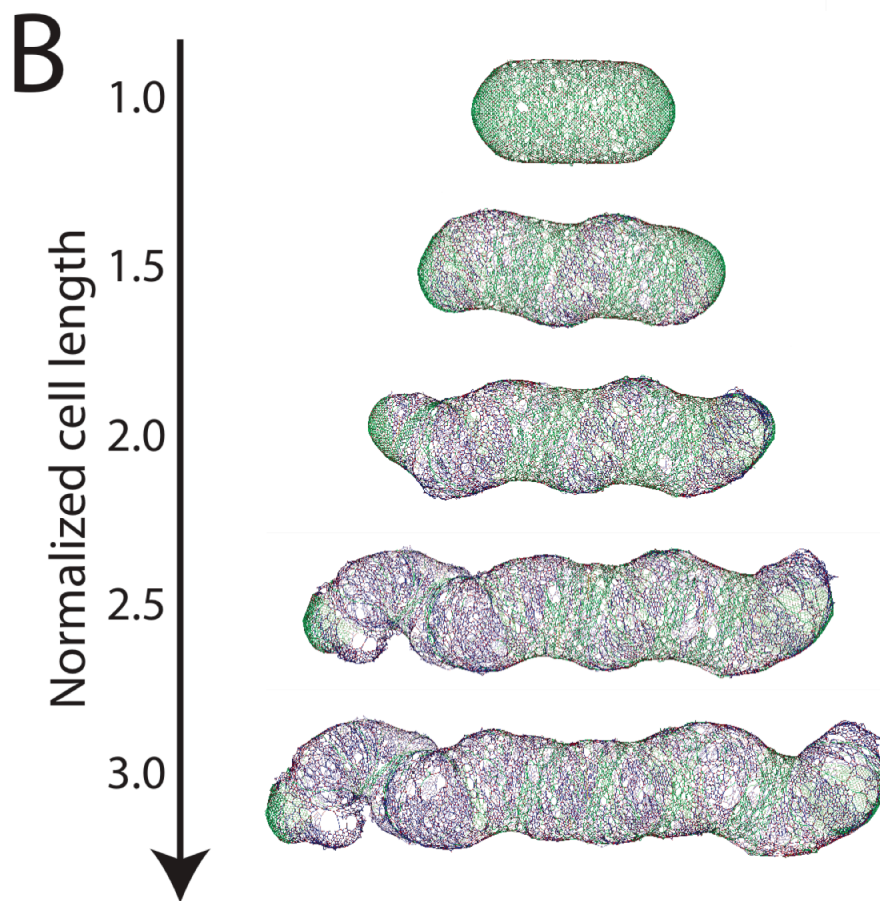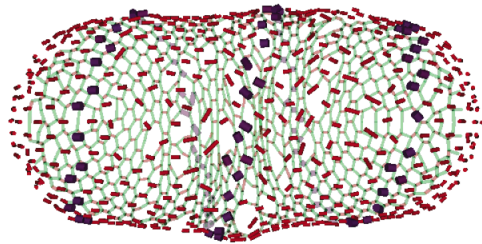
Supplemental Figure 7: Rod shape is poorly maintained for large-pitch helical insertion. (A) Schematic of helical insertion pattern with a helical angle of 30 degrees. Blue shading indicates likelihood of selection as insertion site. (B) Cell wall grown to six times its original length. Increasing the helical pitch causes bulging and irregular width compared with the rod-shaped growth in Fig. 5B.

Supplemental Movies

Supplemental Movie 1 (HuangSI-movie1.avi) shows a typical *E. coli* cell growing on an agarose pad in the presence of 10μg/ml A22. Each frame represents 30 seconds and the movie represents 200 minutes of growth. Initially the cell elongates as it grows, and then begins to round up after the second round of cell division.

Supplemental Movies 2 and 3 (HuangSI-movie2.avi and HuangSI-movie3.avi) show the growth of the cells in Fig. 5D on an agarose pad in the presence of 25μg/ml cephalexin and 10μg/ml A22. Each frame represents 30 seconds. Movie 2 represents 45 minutes of growth and Movie 3 represents 50 minutes of growth. In both cases, the cells elongate as they grow but do not maintain a fixed width.